

Vibrational properties of epitaxial films on metals. I. fcc Cu on the Ni(001) surface

S. Y. Tong, Y. Chen, J. M. Yao, and Z. Q. Wu

Department of Physics and Laboratory for Surface Studies, University of Wisconsin-Milwaukee, Milwaukee, Wisconsin 53201

(Received 8 August 1988)

The general vibrational properties of epitaxially grown fcc Cu films on Ni(001) have been studied using a central-force lattice-dynamical slab model. The theoretical results predicted the emergence of new film modes as the overlayer film's thickness increases. Calculated phonon dispersion curves and spectral densities are presented and the regions of different localizations for the phonon modes in the two-dimensional projected phonon band have been identified.

I. INTRODUCTION

The epitaxial growth of ultrathin films which are pseudomorphic with the substrate has been studied by a number of surface-characterization techniques.¹⁻⁹ In this paper we discuss the general vibrational properties of ultrathin fcc Cu films grown layer by layer (i.e., via the Frank-van der Merwe mechanism) on the Ni(001) surface based on a simple lattice-dynamical model. Since the overlayer (Cu) has a softer force constant than the substrate (Ni), the projected two-dimensional phonon band of Cu occurs at lower frequencies than that of Ni. Questions that we find particularly interesting and for which results are presented below include the emergence of new (film) modes as the overlayer (Cu) film's thickness increases, the rapid damping of the atomic displacement amplitudes in the surface region for the modes whose frequencies lie higher than the maximum $\omega(\mathbf{q})$ of the Cu bulk-phonon band, and the rate of shift in the frequencies of the surface-phonon modes S_4 and S_6 from those of clean Ni to that of Cu as the film grows in thickness.

II. PHONON DISPERSION CURVES OF EPITAXIAL Cu FILMS ON Ni(001)

We first consider the phonon dispersion curves for clean Ni(001), Cu films of various thickness on Ni(001), and clean Cu(001) systems. For simplicity we calculate the phonon dispersions using a nearest-neighbor central-force lattice-dynamical slab model. The force constants suggested by Black *et al.*¹⁰ [i.e., $k_{\text{Cu}}(\text{bulk})=2.81 \times 10^4$ dyn/cm, $k_{\text{Ni}}(\text{bulk})=3.79 \times 10^4$ dyn/cm] are used to describe the Cu-Cu and Ni-Ni interactions. The force constant between Cu and Ni is unknown and we simply take an average of $k_{\text{Ni}}(\text{bulk})$ and $k_{\text{Cu}}(\text{bulk})$, i.e., $k_{\text{Cu-Ni}}=3.3 \times 10^4$ dyn/cm. The spacings between all layers are assumed to be the bulk value of Ni. Obviously, we have chosen extremely simple dynamical and structural models for these systems. The frequencies of some of the phonon modes will shift if more accurate lattice-dynamical or structural models are used. However, the general properties described in the following should remain valid. Indeed, one of the purposes of this analysis is to stimulate experimental measurements of such epitaxially grown films from which the relevant dynamical and structural

parameters can be determined.

The phonon dispersion curves from $\bar{\Gamma}$ to \bar{X} (i.e., along the [110] or \hat{x} direction) for clean Ni(001) are shown in Fig. 1. A slab of 61 atomic layers, with surfaces on either side, is used. At the \bar{X} point the lowest two modes are surface phonons.¹¹ The S_1 mode is shear horizontal with surface (topmost layer) atomic displacement polarized in the $[\bar{1}10]$ or \hat{y} direction. This mode is selection forbidden under normal scattering conditions and will not be discussed further. The S_4 (Rayleigh) mode has surface (topmost layer) atomic displacement polarized in the \hat{z} direction, i.e., normal to the surface, and the mode occurs at 125 cm^{-1} at the \bar{X} point. Experimentally, the S_4 mode at \bar{X} for Ni(001) occurs at 130 cm^{-1} .^{12,13} This value of the S_4 frequency can be obtained in the calculation by increasing the surface force constant which couples atoms

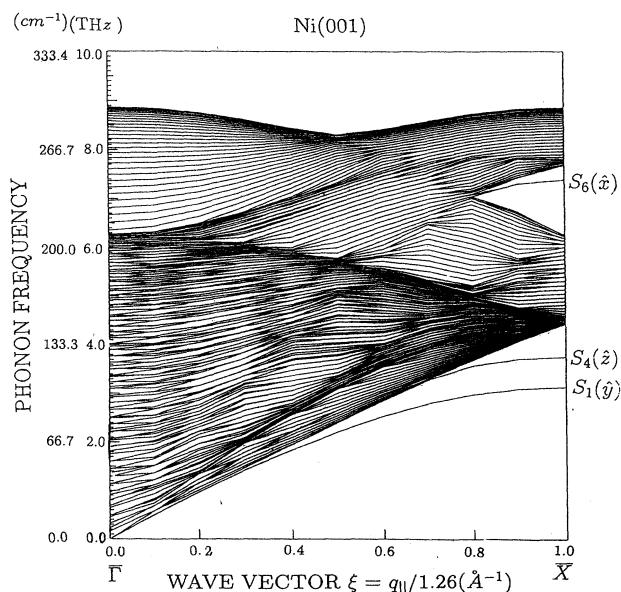


FIG. 1. Calculated phonon dispersion curves between $\bar{\Gamma}$ and \bar{X} for Ni(001) using a nearest-neighbor central-force lattice-dynamical model. The coordinates in the parentheses denote the directions of the surface-layer atomic displacement for the corresponding phonon modes.

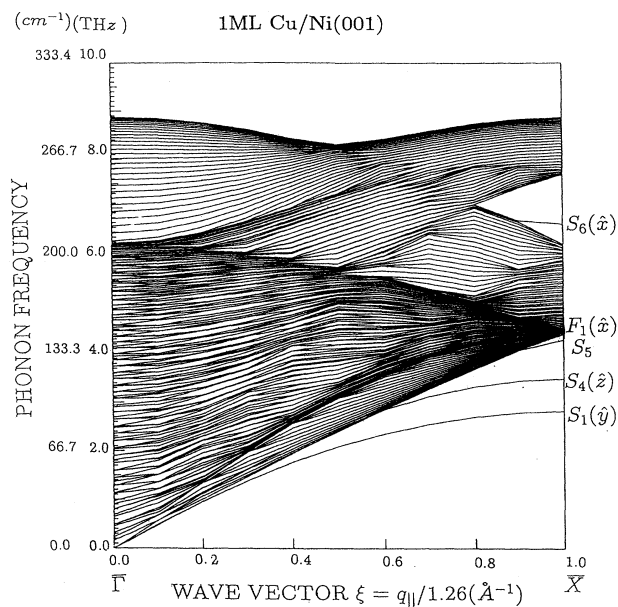


FIG. 2. Similar to Fig. 1 for 1 ML Cu/Ni(001).

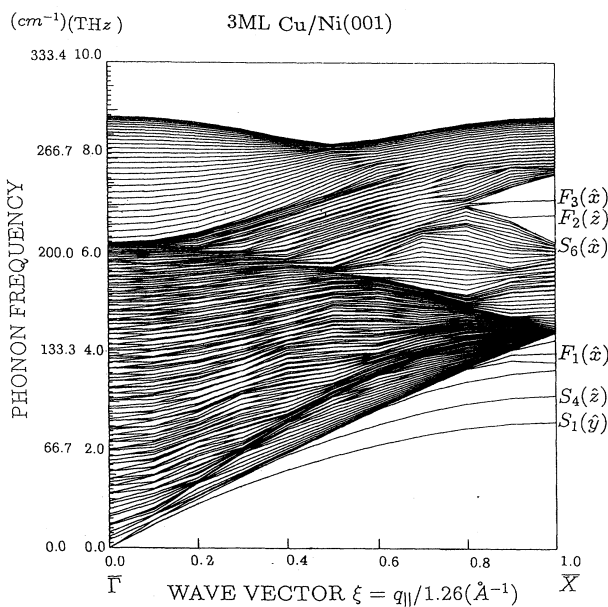


FIG. 4. Similar to Fig. 1 for 3 ML Cu/Ni(001).

in the first layer to those of the second by 20%.¹²⁻¹⁴ For simplicity, such an increase in k_{12} has not been included here. The projected Ni bulk-phonon band at \bar{X} begins at 148 cm^{-1} and has a gap between 206 and 258 cm^{-1} . Inside the gap, the S_6 surface-phonon mode, whose surface (topmost layer) atomic displacement is polarized in the \hat{x} direction, occurs at 247 cm^{-1} . Above the gap, Ni bulk-phonon modes occupy a region between 258 and 295 cm^{-1} .

For a Cu film on the Ni(001) system, a slab of total 61 atomic layers is used and the Cu layers are placed

symmetrically on each side of the slab. The phonon dispersion curves for monolayer and bilayer Cu films on Ni are shown in Figs. 2 and 3, respectively. For the monolayer film case, i.e., 1 ML Cu/Ni(001), both the S_4 and S_6 modes shift to lower frequencies, towards those of clean Cu(001). The S_5 mode appears below the Ni bulk-phonon band, its atomic displacement entirely localized in the second atomic layer. There is a new film mode, we call it the F_1 mode, which appears near the \bar{X} point just below the Ni bulk-phonon band. This mode has its surface atomic displacement along the x direction. For the

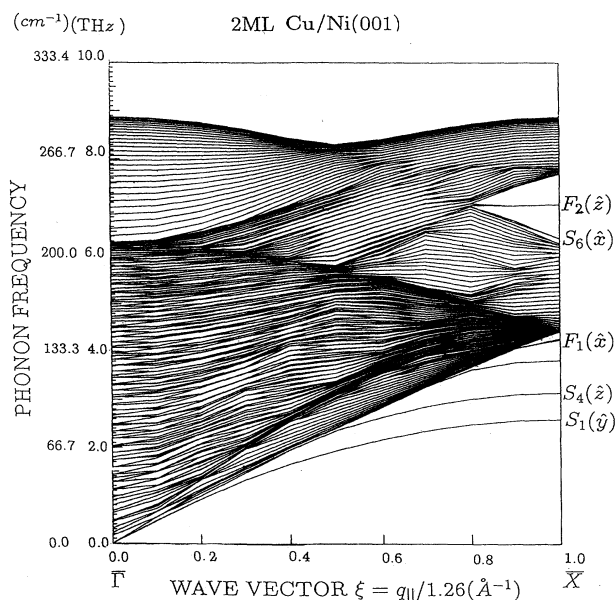


FIG. 3. Similar to Fig. 1 for 2 ML Cu/Ni(001).

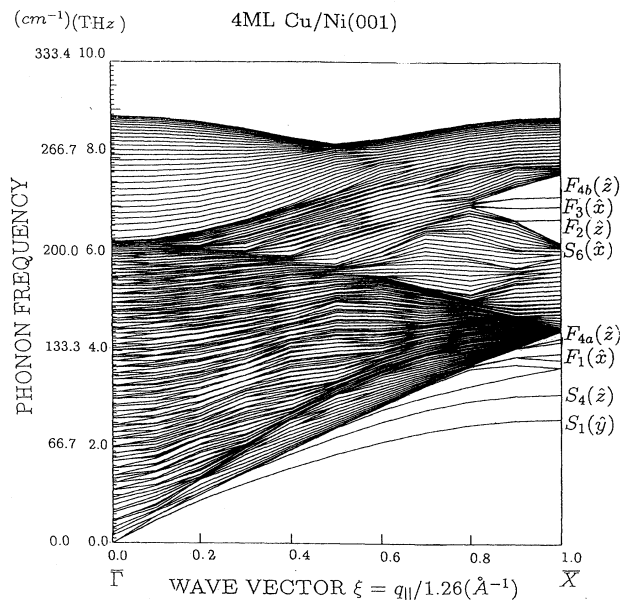


FIG. 5. Similar to Fig. 1 for 4 ML Cu/Ni(001).

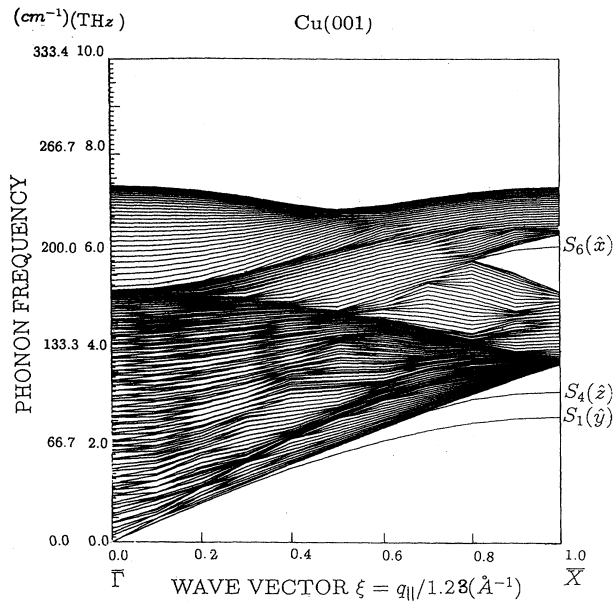
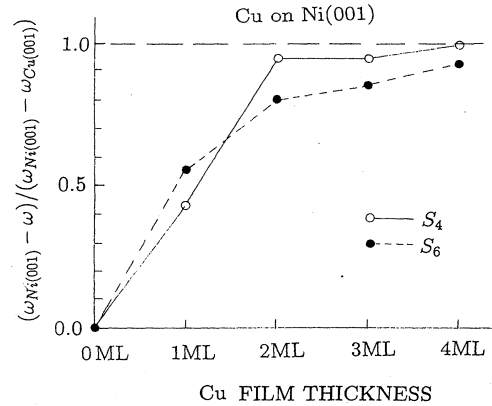


FIG. 6. Similar to Fig. 1 for Cu(001).

bilayer case, i.e., 2 ML Cu/Ni(001), a new film mode, F_2 , appears in the Ni bulk-phonon band gap in addition to the S_6 mode. This mode has its surface atomic displacement along the \hat{z} direction. The dispersion curves for three and four Cu-overlayer films on Ni are shown in Figs. 4 and 5. The phonon dispersions for clean Cu(001) are shown in Fig. 6. For 3 ML Cu/Ni(001) and 4 ML Cu/Ni(001), additional film modes appear below the Ni bulk-phonon band and in its band gap. The surface (topmost layer) atomic displacement of these film modes at the \bar{X} point are indicated in the figures. Only modes with nonzero surface atomic displacements are named in the figures. Comparing the frequencies of the film modes and the phonon band of clean Cu(001) (Fig. 6), we can identify these film modes as the beginning of Cu bulk modes that occupy these frequency regions.

The S_6 surface mode has shifted towards the bottom of the Ni bulk-phonon band gap for 3 ML Cu/Ni(001). For 4 ML Cu/Ni, the S_6 mode is pushed inside the bulk-phonon band of the substrate. The rapid downshift in frequency of S_4 and S_6 surface-phonon modes at \bar{X} from those of clean Ni(001) to that of clean Cu(001) is summa-

FIG. 7. Calculated phonon frequency shifts as a function of Cu film thickness for the S_4 and S_6 surface modes at \bar{X} .

rized in Table I. We note that the shift is over 80% complete at 2 ML thickness. The rates of shift of these two surface modes as a function of overlayer-film thickness are plotted in Fig. 7. The experimentally measured S_4 frequency at \bar{X} for Cu(001) occurs at 108 cm^{-1} .^{15,16} To reproduce this frequency, the surface force constant k_{12} between the first and second copper layers is increased by 16%. Again, for simplicity, we have kept $k_{12} = k_{\text{bulk}}$ here. As a result, the calculated S_4 frequency at \bar{X} for Cu(001) occurs at 104 cm^{-1} .

III. SPECTRAL DENSITIES OF EPITAXIALLY GROWN Cu FILMS ON Ni(001)

The dispersion curves shown in Figs. 1–6 include all the normal modes of the slab. They provide no information as to which modes are localized in either the substrate or the overlayer film. Surface phonons are probed by inelastic helium atom¹⁷ or electron scattering.^{12,18,19} Both techniques preferentially sample atomic displacements in the surface region.¹⁸ To provide a better description of the localization of the modes and to give an indication as to which modes may have large inelastic-He- or electron-scattering cross sections, we plot the spectral density (i.e., the square of the eigenvectors) of the surface (topmost layer) atom for each of the systems considered in the preceding section. The spectral densities of atomic displacements normal to the surface

TABLE I. Calculated frequency shifts of the S_4 and S_6 surface modes at \bar{X} as a function of the film's thickness.

System	Frequency ω (cm^{-1})		$\frac{\omega_{\text{Ni}(001)} - \omega}{\omega_{\text{Ni}(001)} - \omega_{\text{Cu}(001)}} (\%)$	
	S_4 mode	S_6 mode	S_4 mode	S_6 mode
Ni(001)	125	247	0	0
1 ML Cu/Ni	116	223	42.8	55.8
2 ML Cu/Ni	105	212	95.2	81.4
3 ML Cu/Ni	105	210	95.2	86.0
4 ML Cu/Ni	104	207	100.0	93.0
Cu(001)	104	204	100.0	100.0

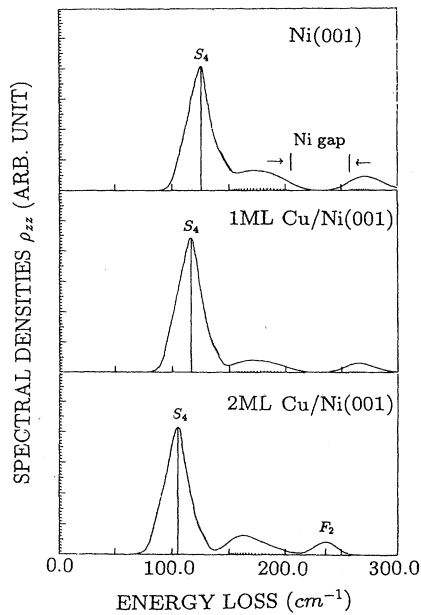


FIG. 8. Surface-atomic-layer spectral densities ρ_{zz} at \bar{X} for Ni(001), 1 ML Cu/Ni(001), and 2 ML Cu/Ni(001).

(i.e., ρ_{zz}) and parallel to the \hat{x} direction (i.e., ρ_{xx}) at the \bar{X} point are shown in Figs. 8–11. In these figures each vertical line represents the ρ_{zz} or ρ_{xx} for an individual mode. The theoretical spectra are obtained by Gaussian broadening each line with a full width at half maximum of 20 cm^{-1} .

We first note the rapid downshift of the frequencies of the S_4 (Figs. 8 and 9) and S_6 (Figs. 10 and 11) modes. From Fig. 11 it is clear that the S_6 mode is shifted in fre-

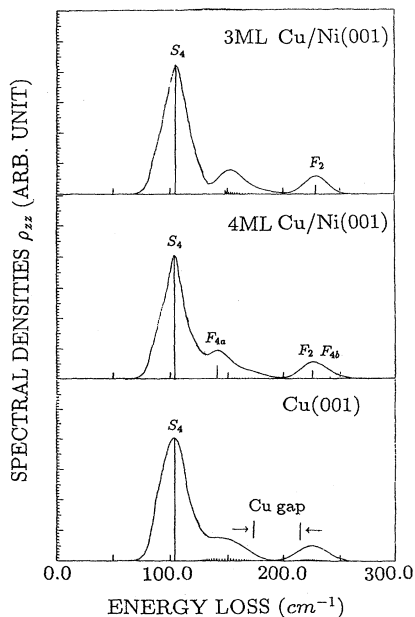


FIG. 9. Similar to Fig. 8 for 3 ML Cu/Ni(001), 4 ML Cu/Ni(001), and Cu(001).

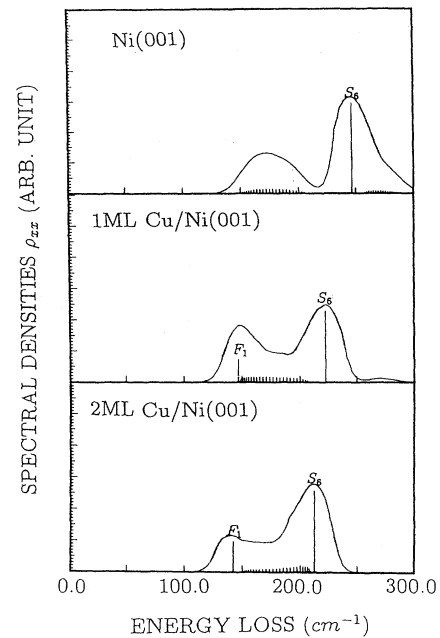


FIG. 10. Surface-atomic-layer spectral densities ρ_{xx} at \bar{X} for Ni(001), 1 ML Cu/Ni(001), and 2 ML Cu/Ni(001).

quency down to the edge of the Ni bulk-phonon band gap for 3 ML Cu/Ni and is inside the Ni bulk-phonon band (however, this is the frequency region of the Cu bulk-phonon band gap) for 4 ML Cu/Ni. A striking feature not evident from the dispersion curves shown in Fig. 3 is that at as little as two monolayers (i.e., 2 ML Cu/Ni) all the bulk-phonon modes above 258 cm^{-1} are damped out at the surface. This fact is clearly evident in the disappearance of ρ_{zz} and ρ_{xx} in Figs. 8 and 10 for the case of 2

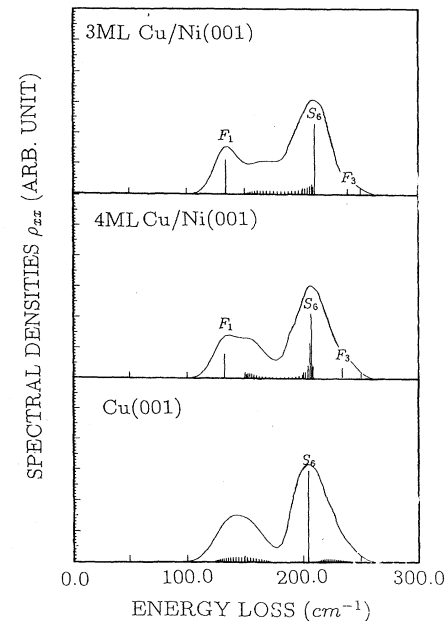


FIG. 11. Similar to Fig. 10 for 3 ML Cu/Ni(001), 4 ML Cu/Ni(001), and Cu(001).

ML Cu/Ni. Our interpretation of this rapid surface atomic displacement damping is that as the Cu film grows in thickness the softer force constant between Cu atoms cannot sustain the high-frequency normal modes of the substrate (Ni) which occur above the top of the Cu bulk-phonon band. Thus, these normal modes are essentially confined to the Ni substrate. Their displacement amplitudes vanish as they penetrate into the Cu film.

Referring back to Figs. 8 and 9, the small peak of ρ_{zz} above 258 cm^{-1} for clean Ni(001) is shifted down to below 250 cm^{-1} at 2 ML of Cu growth. As the Cu film's thickness increases, the number of modes in this region ($206\text{--}258 \text{ cm}^{-1}$) also increases. Since this is the frequency region of the Ni phonon band gap, the atomic displacement of these modes are damped as they go into the substrate. These are localized film modes much of atomic displacements reside within the overlayer film and a few substrate layers. The same is true for film modes that appear below the Ni bulk-phonon band and film modes with surface atomic displacements along the \hat{x} direction (see Figs. 10 and 11, 2 ML Cu/Ni and 3 ML Cu/Ni) that occur in the Ni phonon band gap.

Above, we have seen normal modes of the overlayer which appear in the frequency gap of the substrate. It is known that there is a phonon frequency gap ($171\text{--}213 \text{ cm}^{-1}$) near \bar{X} for clean Cu(001).^{10,15,16} However, for Cu-overlayer films on Ni(001), there are many Ni phonon modes in this region. As Cu atoms are deposited on the Ni substrate, the Ni bulk modes drive the Cu atoms to vibrate at frequencies that fall in the Cu phonon band gap. As the Cu film's thickness increases, the atomic displacements within the Cu film are damped. As a result, the spectral density for 2 ML Cu/Ni and clean Cu are very different in the region of the gap (see Figs. 10 and 11). These substrate-driven resonant film modes persist even at 4 ML thickness. However, the integrated spectral curves for \hat{x} and \hat{z} displacements are already quite similar between 4 ML Cu/Ni and clean Cu. The Cu gap should appear between 5 and 10 ML.

IV. SUMMARY

We have studied the vibrational properties of epitaxially grown Cu films on the Ni(001) surface based on a central-force lattice-dynamical slab model. We can make a few general observations.

(i) The surface modes S_4 and S_6 undergo rapid shifts in their frequencies from those of the clean surface to that of the overlayer material as the overlayer film's thickness grows.

(ii) The atomic displacements of the substrate modes whose frequencies lie above the maximum $\omega(\mathbf{q})$ of the overlayer film are damped out extremely rapidly in the film. This is the strong-substrate-localization (SL) case. For the nearest-neighbor central-force-constant model, the damping is complete at the 2 ML thickness.

(iii) Atoms in the overlayer film may vibrate with fre-

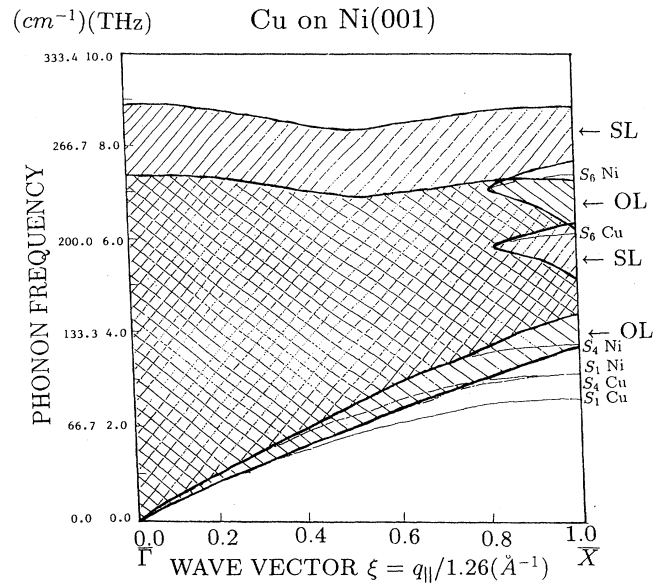


FIG. 12. Superposition of calculated phonon dispersion curves for Ni(001) and Cu(001). The regions of the different localization for the phonon modes are indicated in the figure; "SL" represents substrate localization and "OL" represents overlayer (or film) localization.

quencies which lie inside the phonon band gap of the overlayer material. The atomic displacements of these modes are damped within the overlayer film as the film's thickness increases. We call this the substrate-localization (SL) situation.

(iv) Overlayer film modes that occur in the frequency gap or below the bulk-phonon band of the substrate are damped as their displacements penetrate into the substrate. For these "film" modes, their atomic displacements are localized in the overlayer film and a few top-most substrate layers. This corresponds to the overlayer-localization situation (OL).

In Fig. 12 we depict the regions of different localizations.

Finally, we would like to caution against making direct comparisons of the spectral densities shown in Figs. 8–11 with either inelastic-He- or electron-scattering cross sections. For a given material and wave vector, the spectral densities are fixed, while inelastic-He- or electron-scattering cross sections are functions of incident energy and scattering geometry. In broad terms, inelastic He scattering should be particularly sensitive to the \hat{z} -component spectral density (Figs. 8 and 9), while inelastic electron scattering is sensitive to both the \hat{x} and \hat{z} components.¹⁸ Also, the incident electron penetrates a few atomic layers; hence inelastic-electron-scattering cross sections are sensitive to spectral densities of the first few surface layers (and the phases of the eigendisplacements are important).^{20,21}

In the following paper²² we shall investigate the vibrational properties of epitaxial films whose force constant is stiffer than that of the substrate. This is the case of Ni films on Cu(001) surfaces.

ACKNOWLEDGMENTS

This work was supported by the U.S. Department of Energy under Grant No. DE-FG0284ER45076 and the

Petroleum Research Fund under Grant No. 1154-AC5,6. One of us (Y.C.) acknowledges financial support from the IBM Corporation.

-
- ¹J. P. Biberian and G. A. Somorjai, *J. Vac. Sci. Technol.* **16**, 2073 (1979).
- ²E. Bauer, *Appl. Surf. Sci.* **11**, 479 (1982); E. Bauer and J. H. van der Merwe, *Phys. Rev. B* **33**, 3657 (1986).
- ³Z. Q. Wang, Y. S. Li, F. Jona, and P. M. Marcus, *Solid State Commun.* **61**, 623 (1987); Z. Q. Wang, S. H. Lu, Y. S. Li, F. Jona, and P. M. Marcus, *Phys. Rev. B* **35**, 9322 (1987).
- ⁴S. A. Chambers, T. J. Wagener, and J. H. Weaver, *Phys. Rev. B* **36**, 8992 (1987); S. A. Chambers, S. B. Anderson, H.-W. Chen, and J. H. Weaver, *ibid.* **35**, 2592 (1987).
- ⁵W. F. Egelhoff, Jr., *Phys. Rev. Lett.* **59**, 559 (1987).
- ⁶D. Winfried, *J. Electron Spectrosc. Relat. Phenom.* **44**, 271 (1987).
- ⁷W. Kümmerle and U. Gradman, *Solid State Commun.* **24**, 33 (1977).
- ⁸B. Heinrich, A. S. Arrott, J. F. Cochran, C. Liu, and K. Myrtle, *J. Vac. Sci. Technol. A* **4**, 1376 (1986).
- ⁹W. Keune, K. Halbauer, U. Gonser, J. Lauer, and D. L. Williamson, *J. Appl. Phys.* **48**, 2976 (1977).
- ¹⁰J. E. Black, D. A. Campbell, and R. F. Wallis, *Surf. Sci.* **115**, 161 (1982).
- ¹¹For a review of surface phonons of the fcc (100) face, see, for example, R. E. Allen, G. P. Alldredge, and F. W. de Wette, *Phys. Rev. B* **4**, 1648 (1971); **4**, 1661 (1971), and Ref. 10.
- ¹²S. Lehwald, J. M. Szeftel, H. Ibach, T. S. Rahman, and D. L. Mills, *Phys. Rev. Lett.* **50**, 518 (1983).
- ¹³M. Rocca, S. Lehwald, H. Ibach, and T. S. Rahman, *Surf. Sci.* **138**, L123 (1984).
- ¹⁴M. L. Xu, B. M. Hall, S. Y. Tong, M. Rocca, H. Ibach, S. Lehwald, and J. E. Black, *Phys. Rev. Lett.* **54**, 1171 (1985).
- ¹⁵M. Wuttig, R. Franchy, and H. Ibach, *Solid State Commun.* **57**, 445 (1986).
- ¹⁶L. L. Kesmodel, M. L. Xu, and S. Y. Tong, *Phys. Rev. B* **34**, 2010 (1986).
- ¹⁷J. P. Toennies, *J. Vac. Sci. Technol. A* **2**, 1055 (1984).
- ¹⁸S. Y. Tong, C. H. Li, and D. L. Mills, *Phys. Rev. Lett.* **44**, 407 (1980); C. H. Li, S. Y. Tong, and D. L. Mills, *Phys. Rev. B* **21**, 3057 (1980).
- ¹⁹H. Ibach and D. L. Mills, *Electron Energy Loss Spectroscopy and Surface Vibrations* (Academic, New York, 1982).
- ²⁰S. Y. Tong, Y. Chen, and Z. Q. Wu, *Phys. Rev. B* **38**, 2192 (1988).
- ²¹Y. Chen, Z. Q. Wu, M. L. Xu, S. Y. Tong, K. M. Ho, and X. W. Wang, *Phys. Rev. B* **37**, 9978 (1988).
- ²²Y. Chen, Z. Q. Wu, J. M. Yao, and S. Y. Tong, following paper, *Phys. Rev. B* **39**, 5617 (1989).